J Mater Sci (2007) 42:4675–4683
DOI 10.1007/s10853-006-0372-5

Growth and characterization of high resistivity c-axis oriented ZnO films on different substrates by RF magnetron sputtering for MEMS applications

Ravindra Singh · Mahesh Kumar · Sudhir Chandra

Received: 16 January 2006 / Accepted: 24 April 2006 / Published online: 31 January 2007
© Springer Science+Business Media, LLC 2007

Abstract In the present work, we report the deposition of high resistivity c-axis oriented ZnO films by RF magnetron sputtering. The deposition parameters such as RF power, target-to-substrate spacing, substrate temperature, and sputtering gas composition affect the crystallographic properties of ZnO films, which were evaluated using XRD analysis. The self-heating of the substrate in plasma during film deposition was investigated and we report that highly ‘‘c-axis oriented’’ ZnO thin films can be prepared on different substrates without any external heating under optimized deposition parameters. The post-deposition annealing of the film at 900 °C for 1 h in air ambient increases the intensity of (002) peak corresponding to c-axis orientation in addition with the decrease in full width at half maxima (FWHM). Bond formation of ZnO was confirmed by FTIR analysis. Grains distribution and surface roughness have been analyzed using SEM and AFM. The DC resistivity of the films prepared under different deposition conditions was measured using MIS/MIM structures and was found to be in the range of 10^{11}–10^{12} Ω cm at low electric field of 10^4 V/cm. The ZnO film of 1 μm thickness has transmittance of over 85% in the visible region. Applications of these films in MEMS devices are discussed.

R. Singh · M. Kumar · S. Chandra (✉)
Centre for Applied Research in Electronics (CARE), Indian Institute of Technology Delhi, Hauz Khas, New Delhi 110016, India
e-mail: schandra@care.iitd.ernet.in

Introduction

In the recent years, extensive research has been carried out on zinc oxide (ZnO) thin films because of their applications in surface acoustic wave (SAW) devices, bulk acoustic wave (BAW) resonators, optical waveguides, transparent conducting coatings, light emitting diodes (LED), photodetectors and electroluminescence devices [1–7]. These films can also be used in Micro Electro Mechanical Systems (MEMS) as a sensing material because of their piezoelectric properties [8] and as sacrificial layer in surface micromachining [9].

Various techniques are reported for the deposition of ZnO thin films, such as sputtering [10], evaporation [11], chemical vapor deposition [12], sol-gel [13], spray pyrolysis [14], pulsed laser deposition [15], atomic layer deposition [16], vacuum arc deposition [17] and molecular beam epitaxy [18]. Among these techniques, sputtering is the preferred method as oriented and uniform films can be obtained even at relatively low substrate temperatures [10].

For applications of ZnO films based on its piezoelectric properties, it is a requirement that the films should be ‘‘c-axis oriented’’ and have high resistivity. For SAW and other devices using ZnO, films up to several micron thickness are required on various substrates [19]. Furthermore, ZnO films deposition at comparatively low temperature is of great interest for realization of MEMS in post-CMOS processing procedures. The aim of the present investigation is to obtain high deposition rates for preparing high resistivity and c-axis oriented ZnO films at low deposition temperatures. Most of the research papers published earlier describe the deposition of low resistivity (~0.1 Ω cm) c-axis oriented ZnO

thin films at 200–500 °C substrate temperature [20, 21]. A few recent publications have reported the preparation of c-axis oriented ZnO thin films below 200 °C [22, 23].

In the present work, high resistivity ''c-axis oriented'' ZnO thin films have been prepared on different substrates by RF magnetron sputtering. The effect of substrate temperature, RF power, target-to-substrate spacing, and sputtering gas composition has been investigated on the structural properties of the films. We report in this paper that self-heating of the substrate during sputtering process is sufficient to prepare c-axis oriented ZnO thin films. The structural, electrical and optical properties of these films have also been investigated.

Experimental work

ZnO thin films were deposited on glass, Si (100), SiO_2 (1 μm)/Si, p^+(4 μm)-Si, Au(250 nm)/Cr(50 nm)/SiO_2 (1 μm)/Si, Cu(300 nm)/Si, Al(400 nm)/Si and Pt (150 nm)/Ti(30 nm)/SiO_2(1 μm)/Si substrates by RF magnetron sputtering in ''sputter-up configuration'' using a 75 mm diameter and 5 mm thick ZnO target (99.99% purity). The diameter and the thickness of the silicon wafers used were 2 in and 280 μm, respectively. The glass substrate was 1 mm thick in square shape (1″ × 1″). Before deposition, the substrates were thoroughly cleaned using standard cleaning processes for different materials. In order to investigate the effect of target to substrate spacing, sputtering gas, RF power, deposition temperature and post-deposition annealing on crystallographic orientation of ZnO, a number of films were prepared on Si (100) substrates under different deposition conditions. The chamber was evacuated to 1×10^{-5} Torr pressure before introducing the sputtering gas. Sputtering was carried out in (i) pure argon and (ii) mixture of oxygen and argon (1:1) by supplying 100–200 W RF power at a frequency of 13.56 MHz. The flow rates of both the argon and oxygen were controlled by rotameters. The sputtering pressure was maintained at 10 mTorr for all the depositions. The distance between the target and the substrate was varied between 40 mm and 60 mm. The substrates could be heated (if required) up to 300 °C by a 500 W halogen lamp mounted in the substrate holder. The temperature was monitored and controlled using a thermocouple attached to the substrate. The substrate holder was designed to minimize the heat loss to the chamber. This enabled the substrate temperature to rise during sputtering process even when no external heating was used. The sputtering parameters used for preparing ZnO thin films are summarized in Table 1.

Table 1 Sputtering conditions used for the preparation of ZnO films

Deposition parameter	Conditions
RF power	100 W, 150 W, and 200 W
Sputtering gas	Ar and Ar–O_2 mixture (1:1)
Sputtering pressure	10 m Torr
Target-to-substrate distance	40 mm, 50 mm, and 60 mm
Substrate temperature	(i) External heating (up to 300 °C) (ii) Pre-heating to 110 °C, heater switched off before starting sputtering. (iii) No external heating, only self-heating by plasma

In order to investigate the crystallographic properties of the ZnO thin films, X-ray diffraction (XRD) analysis was carried out on PW 3040 Philips X'Pert X-ray diffractometer using CuK_α (λ = 1.5405 Å) radiation. The infrared spectra were recorded by a Perkin-Elmer FTIR spectrometer in the range 400–4,000 cm^{-1} using a bare silicon wafer as a reference. The surface morphology and the root-mean-square (rms) surface roughness of the films were characterized using scanning electron microscope (SEM) and atomic force microscope (AFM). The thickness of the films was determined using surface profiler (Tencor Instruments). The step was formed by lithography and etching of the film in 1% HCl solution. For the measurement of resistivity of the films, aluminum electrodes of area 0.442 mm^2 were formed by thermal evaporation using a sheet metal mask. The dc resistivity was measured using a computer interfaced Keithley 2410, source meter. For optical/UV transmission spectra, films were deposited on glass substrates. The spectra were obtained using a Perkin-Elmer Lambda 900 UV-VIS-NIR spectrophotometer.

Results and discussion

The substrate temperature during the sputter-deposition process is known to have a pronounced effect on crystallographic properties of ZnO [10, 21]. It is well known that, during the sputtering process, the substrate temperature rises [24]. We have investigated whether this self-heating phenomenon can be exploited to obtain c-axis oriented ZnO growth. Figure 1 shows the change in substrate temperature with time during the sputtering (RF power: 100 W, target-substrate distance: 40 mm, 50 mm, and 60 mm) when no external heating was provided. The temperature rises

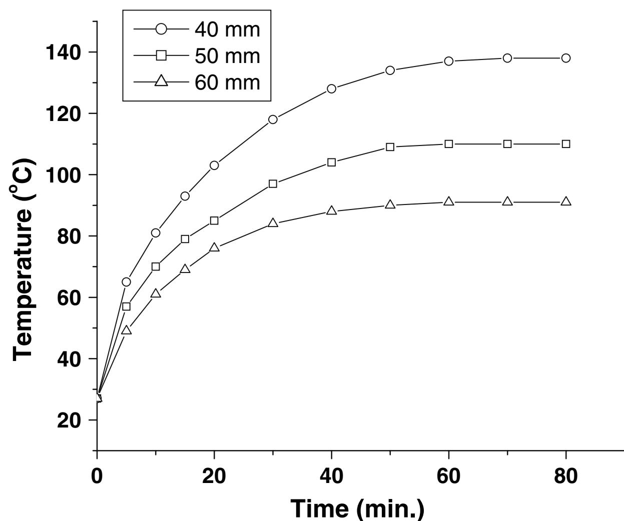

Fig. 1 Change in substrate temperature with time during the sputtering at different target-to-substrate spacings (RF power: 100 W). No external heating was provided

gradually and stabilizes in about 50 min time. The maximum substrate temperature is a function of target-to-substrate spacing. For the 40 mm, 50 mm and 60 mm spacing, its value is 138 °C, 110 °C, and 90 °C, respectively.

Figure 2 shows the XRD pattern of ZnO thin films (thickness ~ 1 μm) deposited on silicon substrate with no external heating in (i) pure argon and (ii) mixture of argon and oxygen (1:1). The target-to-substrate spacing was 50 mm. In both the cases, (002) peaks are predominant indicating c-axis oriented film growth. However, the film prepared in pure argon shows additional low intensity peaks whereas for the films formed in $Ar\text{-}O_2$, only (002) peak is present. The corresponding 2θ values (34.131° and 34.283°, respectively) are somewhat lower compared to the value for the bulk ZnO (34.44°) [25], indicating the presence of tensile stress. It is noteworthy that the addition of oxygen during sputtering process eliminates other unwanted peaks from the XRD spectrum. As expected, the deposition rate is slightly reduced in $Ar–O_2$ mixture as compared to that of sputtering in pure argon. It is postulated that the films formed in pure argon have oxygen deficiency resulting in distortion in the lattice structure and appearance of undesired peaks in the XRD spectra. The addition of oxygen in the sputtering gas restores the stoichiometry of the deposited film and improves the c-axis orientation.

In order to investigate the effect of target to substrate spacing on deposition rate, uniformity and crystallographic orientation, ZnO films were prepared at different target to substrate spacing. Figure 3 shows the deposition rate at different target-to-substrate spacing as a function of distance from the center on 2-in silicon wafer. The $Ar–O_2$ (1:1) mixture was used during the sputtering. The deposition rate decreases by increasing the target to substrate spacing whereas the thickness uniformity increases across a 2-in wafer. Figure 4 shows the XRD pattern of ZnO thin films prepared at different target-to-substrate spacings (100 W, $Ar–O_2$ 1:1). In this case, the thickness of the films was kept constant (~1 μm). It reveals that the orientation of ZnO depends weakly on the target-to-substrate spacing. The XRD for the film deposited at 50 mm separation shows the (002) plane only. On the other hand, the films deposited at 40 mm and 60 mm separations have additional peaks as well. The intensity of (002) peak reduces significantly as the spacing increases from 50 mm to 60 mm. This is due to the effect of reduction in the substrate temperature from

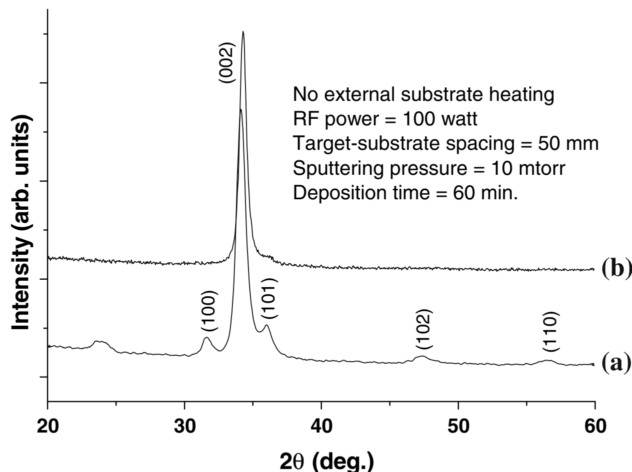

Fig. 2 XRD pattern of ZnO thin films deposited in (**a**) pure argon and (**b**) mixture of argon and oxygen (1:1)

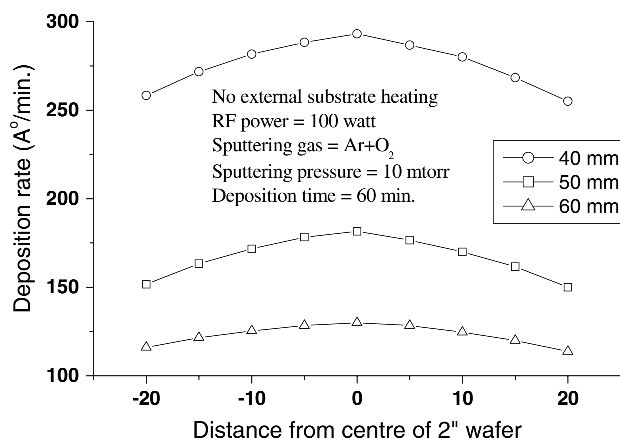

Fig. 3 Deposition rate at different target-to-substrate spacing as a function of distance from the center on a 2-in silicon wafer

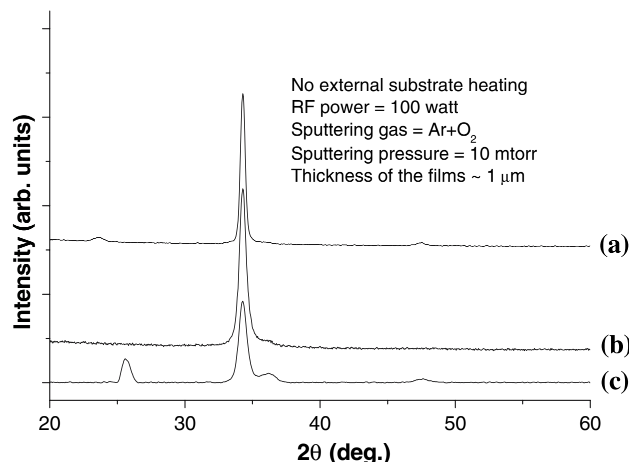

Fig. 4 XRD pattern of ZnO thin films prepared at (**a**) 40 mm, (**b**) 50 mm and (**c**) 60 mm, target to substrate spacing

110 °C to 90 °C, which may not be sufficient for the preferential c-axis (002) growth of the film. The full width at half maximum (FWHM) values of (002) peak were found to be almost identical for 40 mm (0.48°) and 50 mm (0.49°) spacing. For the 60 mm spacing, somewhat higher value of FWHM (0.59°) was observed. However, these values are still well within the limit of 7° required for large effective coupling factor [10]. From the above results, it can be concluded that the film deposited at 50 mm separation is the best as far as the c-axis (002) orientation is concerned. The film deposited at 40 mm separation is also c-axis oriented but two additional minor peaks are also observed. The film deposited at 60 mm spacing is weakly c-axis oriented. It may also be emphasized that the deposition rate for the 40 mm spacing (~277 Å/min) is substantially higher compared to that of 50-mm spacing (~167 Å/min) and 60-mm spacing (~95 Å/min). For applications requiring larger thickness of the ZnO film, this may be a significant consideration [19].

The orientation of ZnO film was investigated as a function of deposition temperature and post-deposition annealing. For this study, the films were deposited at 100 W power in Ar–O_2 (1:1) ambient and the target-to-substrate spacing was fixed at 50 mm. The deposition time was 60 min for all the films. The films were prepared at four different substrate temperatures namely: (a) no external heating, the substrate temperature rises gradually to 110 °C (in plasma) as shown in Fig. 1, (b) preheating at 110 °C and the heater switched off during deposition process, (c) 200 °C and (d) 300 °C. The corresponding XRD patterns of these samples are shown in Fig. 5(a–d). The results are summarized in Table 2. It is evident that a single strong (002) peak corresponding to c-axis orientation appeared at 2θ = 34.282° for the film prepared without external heating of the substrate (Fig. 5a). The FWHM value was found to be 0.492°. For the pre-heated substrate (Fig. 5b), although the intensity of (002) peak was somewhat higher but other unwanted peaks also appeared. On further increasing the deposition temperature to 200° and 300°, the intensity of (002) peak further decreased and other unwanted peaks also appeared. Figure 5(e) shows the XRD of a film prepared without external substrate heating and subsequently annealed in air at 900 °C for 1 h. The peak

Table 2 Crystallographic properties of ZnO films prepared under different sputtering conditions

Sputtering gas	Target-to-substrate spacing (mm)	RF power (W)	Substrate temperature during deposition	Average deposition rate (Å/min)	(002) peak position, 2θ (°)	FWHM (°)	Additional planes [other than (002)]
Pure Ar	50	100	No external heating	185	34.131	0.64	(100), (101), (102), (110) and 1 unidentified plane
Ar + O_2 (1:1)	50	100	No external heating	167	34.282	0.492	Nil
Ar + O_2 (1:1)	40	100	No external heating	277	34.29	0.48	(102) and 1 unidentified plane
Ar + O_2 (1:1)	60	100	No external heating	95	34.253	0.59	(101), (102) and 1 unidentified plane
Ar + O_2 (1:1)	50	150	No external heating	283	34.374	1.181	(100), (101), (102) and 1 unidentified plane
Ar + O_2 (1:1)	50	200	No external heating	455	34.276	0.59	(101), (102) and 1 unidentified plane
Ar + O_2 (1:1)	50	100	Pre-heating at 110 °C	167	34.254	0.541	2 unidentified planes
Ar + O_2 (1:1)	50	100	200 °C	167	34.308	0.64	1 unidentified plane
Ar + O_2 (1:1)	50	100	300 °C	167	34.325	0.852	(100), (101), (102) and 1 unidentified plane
Ar + O_2 (1:1)	50	100	No external heating[a]	167	34.49	0.236	Nil

[a] The sample was subjected to post-deposition annealing at 900 °C for 1 h in air

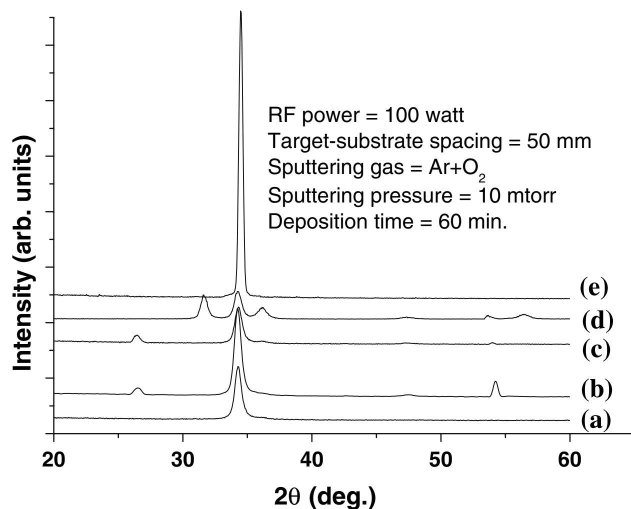

Fig. 5 XRD pattern of ZnO films prepared at different substrate temperatures: (**a**) without external heating, (**b**) pre-heating at 110 °C and the heater switched off during sputtering process, (**c**) external heating to maintain 200 °C and (**d**) external heating to maintain 300 °C, (**e**) the film prepared without external substrate heating followed by furnace annealing at 900 °C for 1 h

height increases dramatically and the FWHM of (002) peak decreases from 0.492° to 0.236° after annealing which indicates significant improvement in the crystallinity of the film. Furthermore, the 2θ value of (002) peak shifted from 34.282° to 34.49°, which is closer to the value corresponding to the bulk ZnO (34.44°) although the stress also changes from tensile to compressive after annealing. It may be emphasized that the ZnO film subjected to post-deposition annealing shows the best possible characteristics in terms of XRD peak (002) position, intensity and FWHM amongst all the samples investigated.

Figure 6 shows the XRD pattern of ZnO films prepared at different RF powers in argon–oxygen mixture without external substrate heating. The target to substrate separation was 50 mm in all the cases. It is confirmed from the figure that c-axis oriented ZnO film was formed at 100 W RF power. The deposition rate and intensity of (002) peak increased by increasing the RF power but other unwanted peaks also appeared. The FWHM values for the 100 W, 150 W, and 200 W powers are: 0.492°, 1.181°, and 0.591°, respectively. From these results, it can be inferred that the ZnO film prepared in Ar + O_2 (1:1) without external substrate heating at 100 W RF power and 50 mm target-substrate spacing is highly c-axis oriented. However, the deposition rate at 200 W power (455 Å/min) is substantially higher compared to that of 100 W power (167 Å/min). The FWHM (0.59°) value is well within the requirement of highly oriented films. For applications requiring

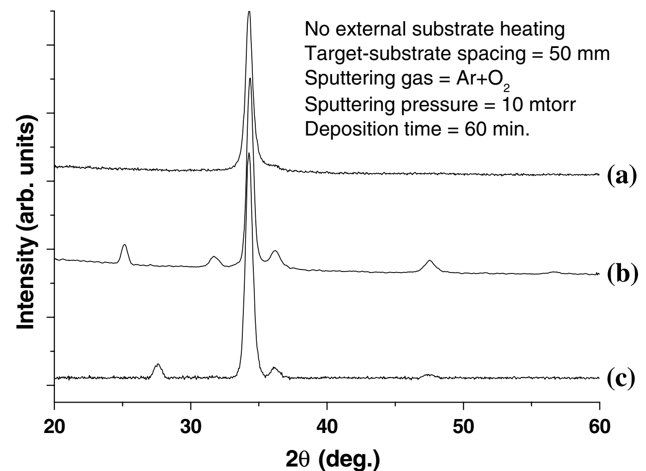

Fig. 6 XRD pattern of ZnO films prepared at (**a**) 100 W, (**b**) 150 W and (**c**) 200 W, RF powers

thicker films, these deposition parameters may be advantageously used.

Figure 7 shows the XRD pattern of ZnO films prepared on a variety of substrates such as glass, Si (100), SiO_2/Si, p^+-Si (heavily boron diffused), Au/Cr/SiO_2/Si, Cu/Si, Al/Si and Pt/Ti/SiO_2/Si. These films were prepared using optimized sputtering parameters (100 W RF power, 50 mm target to substrate spacing, 10 mtorr sputtering pressure, mixture of argon–oxygen 1:1, no external substrate heating). The results are summarized in Table 3. It can be seen that the strong (002) peak corresponding to c-axis orientation appeared for all films. All the additional peaks were identified to be from the substrate. The intensities of

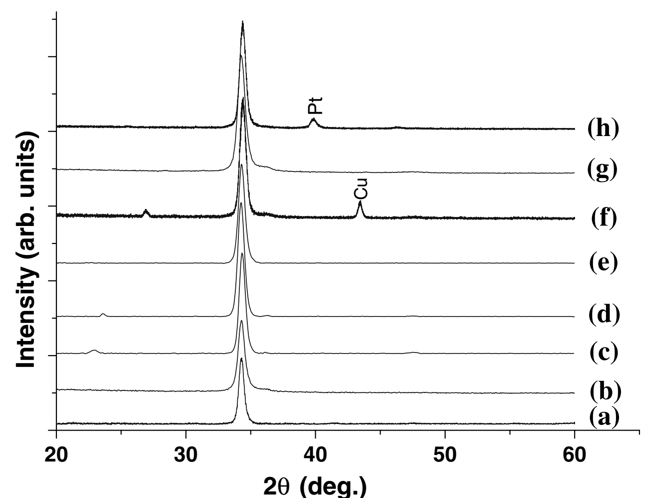

Fig. 7 XRD pattern of ZnO films prepared using optimized sputtering parameters on various substrates: (**a**) glass, (**b**) Si (100), (**c**) SiO_2/Si, (**d**) p^+-Si, (**e**) Au/Cr/SiO_2/Si, (**f**) Cu/Si, (**g**) Al/Si, and (**h**) Pt/Ti/SiO_2/Si

Table 3 The (002) peak positions and FWHM of ZnO films prepared on different substrates using optimized deposition parameters

Substrate	Glass	Si (100)	SiO_2 /Si	p^+-Si (heavily boron diffused)	Au/Cr/SiO_2/Si	Cu/Si	Al/Si	Pt/Ti/SiO_2/Si
(002) peak position, 2θ (°)	34.275	34.283	34.337	34.252	34.296	34.391	34.268	34.407
FWHM (°)	0.312	0.492	0.541	0.612	0.66	0.315	0.72	0.306

the (002) peaks were not much different for these films. However, the FWHM varied from 0.3° to 0.72° and were minimum (~0.3°) in the case of glass, Cu/Si and Pt/Ti/SiO_2/Si substrates. The 2θ values of (002) peak of the films prepared on Cu/Si and Pt/Ti/SiO_2/Si substrates were found to be 34.391° and 34.407°, respectively, which are closer to the value corresponding to the bulk ZnO (34.44°). This indicates that these films have lower tensile stress than the films prepared on other substrates. Very recently Kang et al. [23] reported that only Al and Au coated silicon substrates enhance the growth of c-axis orientation in ZnO films and they did not observe any preferential c-axis growth in the case of Cu/Si and Si substrates. However, some other authors reported the preferential c-axis growth of ZnO films on Si, SiO_2/Si substrates either with or without substrate heating [21, 26]. From our results it can be concluded that all substrates used in the present study support the preferential c-axis growth of ZnO films without external substrate heating. This significantly enhances the choice of the substrates for varied applications requiring piezoelectric ZnO films.

FTIR measurement was performed in order to verify the bond structure of ZnO film prepared using optimized parameters. Figure 8 shows the infrared absorption spectra of bare silicon, as deposited ZnO/silicon and annealed ZnO/silicon in the 4,000–400 cm^{-1} wave-number range. Both as-deposited and annealed ZnO/silicon samples exhibit an absorption peak at 415 cm^{-1}. This matches with the reported value corresponding to Zn–O stretching vibration for a tetrahedral surrounding of zinc atoms for powder sample of ZnO [27]. The other absorption peaks are from silicon substrate. The intensity of Si–O peak was found to increase after annealing, which is due to some oxide growth on the back side of silicon wafer during annealing at 900 °C in air.

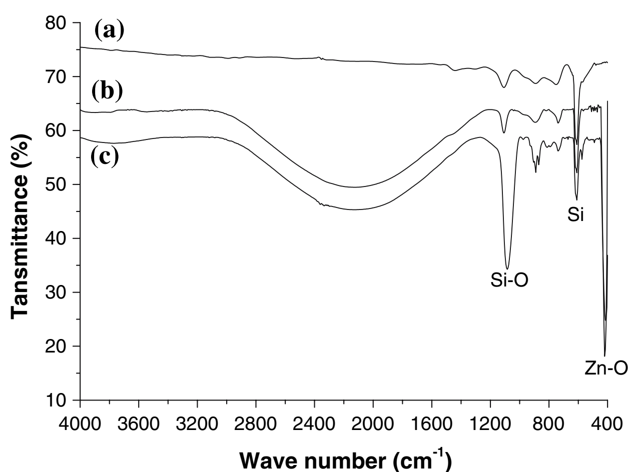

Fig. 8 FTIR absorption spectrums of (**a**) bare silicon, (**b**) as deposited and (**c**) annealed at 900 °C for 1 h. The ZnO films were prepared on silicon at 100 W without external substrate heating in Ar + O_2

The surface morphology was investigated for the as-deposited and annealed ZnO films, which were prepared using optimized sputtering parameters for c-axis orientation. Figure 9 shows the plan view SEM images of these films. It appears from the figure that the grains of the as-deposited film are uniformly distributed with nearly uniform size. This is further confirmed by AFM, shown in Fig. 10. The average grain size calculated from AFM was found to be 147 nm and 411 nm for as-deposited and annealed films, respectively. Although the average grain size increased after annealing, the non-uniformity in the grain size also increased. The rms roughness was found to be 4.865 nm and 9.679 nm for as-deposited and annealed films, respectively. These studies confirm that smooth ZnO films with uniform grain distribution can be prepared without external substrate heating. The annealing at 900 °C for 1 h enhances the grain size of the film.

Figure 11 shows the *I–V* characteristics of ZnO films prepared under different deposition conditions namely: (i) without external substrate heating on Si substrate, (ii) with pre-heating of the substrate at 110 °C on Si substrate, (iii) without external substrate heating on silicon substrate and annealed at 900 °C for 1 h in air, and (iv) without external substrate heating on Al/Si substrate. The first three measurements were done on metal insulator semiconductor (MIS) structures and the last one was done on metal insulator metal (MIM) structure. In the case (i), (ii) and (iv), it is observed that the current follows ohmic behavior ($I \propto V$) at low fields and square-law ($I \propto V^2$) dependence in the higher field region. On further increasing the voltage,

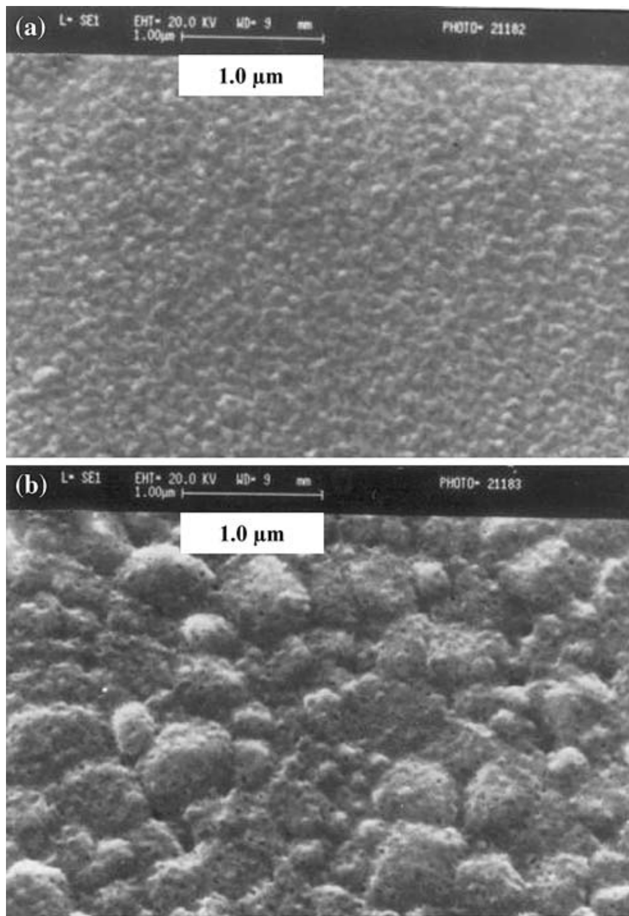

Fig. 9 Plan view SEM of (**a**) as deposited and (**b**) annealed at 900 °C for 1 h. The ZnO films were prepared at 100 W without external substrate heating in Ar + O_2

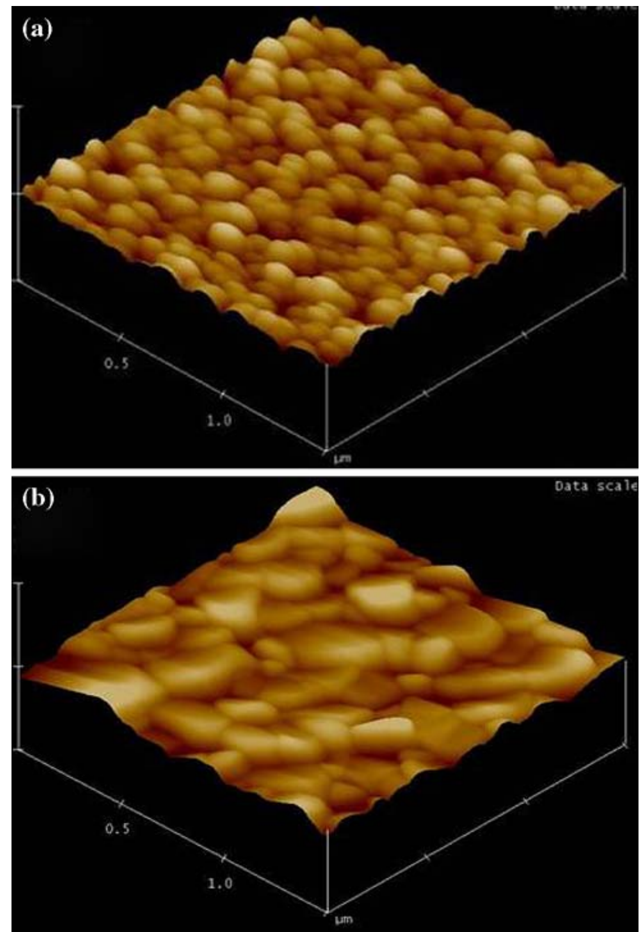

Fig. 10 3-D AFM of (**a**) as deposited and (**b**) annealed at 900 °C for 1 h. The ZnO films were prepared at 100 W without external substrate heating in Ar + O_2

a region of $I \propto V^n$, with n upto 5 was also observed. This nature of log (I) vs. log (V) plots is the characteristic of materials having single-carrier space charge limited (SCL) injection current flow mechanism controlled by shallow trap levels which are distributed in energy, as described by Kao and Hwang [28]. However, in the case of annealed film, the ohmic region extends upto much higher fields and the square-law region was absent. Further increase in the field causes the current to increase very rapidly. Kao and Hwang suggested that higher concentration of traps increases the field at which the transition from ohmic to SCL conduction occurs. In our samples, the annealing results in increase in grain size, which presumably increases the trap density. This is responsible for shift in ohmic region towards higher fields. In addition, absence of square-law region in the annealed film indicates that the SCL current is controlled by deep trap levels rather than shallow traps [28]. The DC resistivity of the films, calculated from I–V measurements, was found to be in the range of 10^{11}–10^{12} Ω cm at low electric fields (~10 kV/cm). This is much higher than the reported values [29, 30].

The wavelength dependence of optical transmittance spectra of the ZnO film prepared at optimized sputtering parameters is shown in Fig. 12(a). The film having one-micron thickness showed a maximum transmittance of over 85% in the visible region from 450 nm to 650 nm which is better in comparison to other published results [26]. The optical absorption coefficient (α) was evaluated from the transmittance data. The optical band gap values are obtained by extrapolating the linear portion of the plots of $(\alpha h\nu)^2$ versus $h\nu$ to $\alpha = 0$ as shown in Fig. 12(b). The optical band gap energy is found to be 3.34 eV, which closely matches with the values reported by others [31].

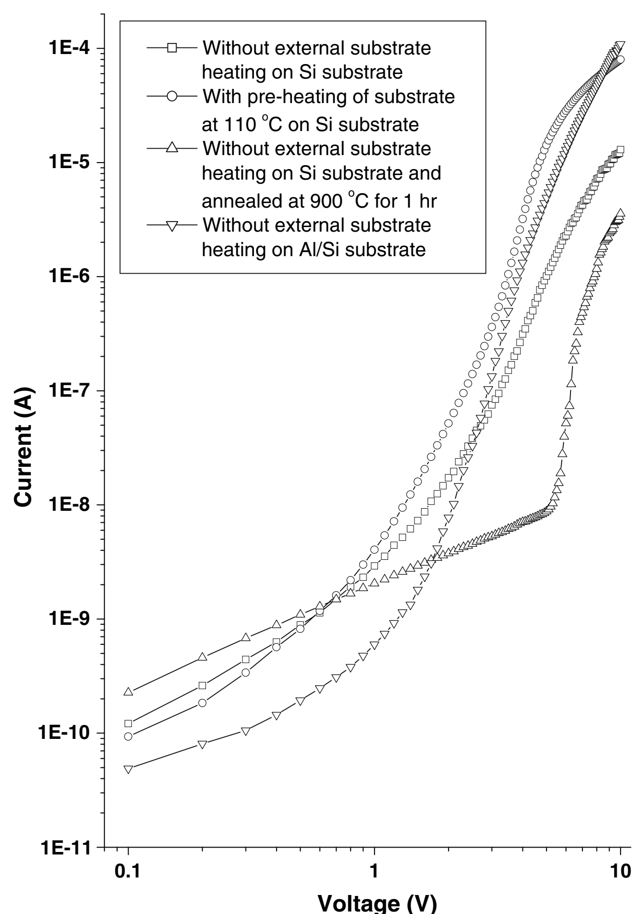

Fig. 11 *I–V* characteristics of ZnO films prepared under different deposition conditions at 100 W in Ar + O_2

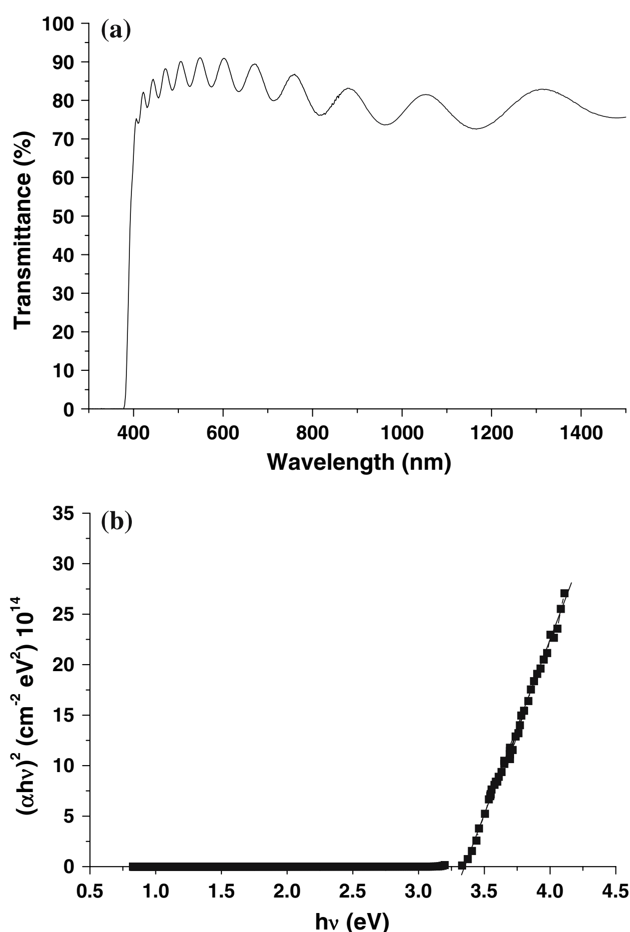

Fig. 12 (**a**) Wavelength dependence of optical transmittance and (**b**) variation of $(\alpha h\nu)^2$ with photon energy ($h\nu$), of ZnO film prepared at 100 W without external substrate heating in Ar + O_2

Conclusion

We have investigated the deposition of ZnO films by RF magnetron sputtering. The orientation and crystallinity of ZnO thin films depend on RF power, target to substrate spacing, sputtering gas and substrate temperature. Highly c-axis orientated ZnO thin films were prepared on various substrates without external substrate heating at 100 W RF power, 50 mm target to substrate spacing, 10 mtorr sputtering pressure in the mixture of argon–oxygen (1:1). The intensity of (002) peak corresponding to c-axis orientation increases and the FWHM decreases after the post-annealing of the film at 900 °C for 1 h. SEM and AFM images reveal the uniform grain distribution of smooth ZnO films. The film has transmittance of over 85% in the visible region from 450 nm to 650 nm. The films prepared under different deposition parameters exhibit high resistivity in the range of 10^{11}–10^{12} Ω cm at low electric field of 10^4 V/cm.

The preparation of highly c-axis oriented films without external substrate heating is advantageous in terms of simpler system design and higher throughput. Furthermore, it has been demonstrated that these films can be formed at substantially higher deposition rates under optimized deposition parameters. This is of particular interest in applications requiring relatively thicker films. These films can be advantageously used in piezoelectric based MEMS devices, e.g., SAW devices, BAW resonators, pressure sensors, vibration sensors, etc. For these applications, the resistivity of the film plays a critical role and high resistivity films are desired. In addition, for SAW devices and BAW resonators, highly c-axis oriented ZnO films on different substrates are required. Therefore, the ZnO films prepared in the present study are suitable for the above applications.

Acknowledgement The work was carried under a Sponsored Research Project of DRDO, Government of India.

References

1. Yamamoto T, Shiosaki T, Kawabata A (1980) J Appl Phys 51:3113
2. Soki T, Hatanaka Y, Look DC (2000) Appl Phys Lett 76:3257
3. Liu Y, Gorla CR, Liang S, Emanetoglu N, Lu Y, Shen H, Wraback M (2000) J Electron Mater 29:60
4. Ferblantier G, Mailly F, Asmar RA, Foucaran A, Delannoy FP (2005) Sensors Actuators A 122:184
5. Devoe DL (2001) Sensors Actuators A 88:263
6. Lee SS, White RM (1998) Sensors Actuators A 71:153
7. Gabl R, Feucht HD, Zeininger H, Eckstein G, Schreiter M, Primig R, Pitzer D, Wersing W (2004) Biosensors Bioelectr 19:615
8. Xu T, Wu G, Zhang G, Hao Y (2003) Sensors Actuators A 104:61
9. Bhatt V, Pal P, Chandra S (2005) Surface Coat Technol 198(1–3):304
10. Ondo-Ndong R, Pascal-Delannoy F, Boyer A, Giani A, Foucaran A (2003) Mater Sci Eng B 97:68
11. Gordillo G, Calderon C (2001) Solar Energy Mater Solar Cells 69:251
12. Li BS, Liu YC, Shen DZ, Zhang JY, Lu YM, Fan XQ (2003) J Cryst Growth 249:179
13. Lee JH, Ko KH, Park BO (2003) J Cryst Growth 247:119
14. Ayouchi R, Martin F, Leinen D, Ramos-Barrado JR (2003) J Cryst Growth 247:497
15. Zeng JN, Low JK, Ren ZM, Liew T, Lu YF (2002) Appl Surf Sci 197:362
16. Yamada A, Sang B, Konagai M (1997) Appl Surf Sci 112:216
17. Xu XL, Lau SP, Chen JS, Sun Z, Tay BK, Chai JW (2001) Mater Sci Semicond Proc 4:617
18. Iwata K, Fons P, Niki S, Yamada A, Matsubara K, Nakahara K, Tanabe T, Takasu H (2000) J Cryst Growth 214/215:50
19. Sharma P (June 2002) PhD Dissertation, Ch. 4, Department of Physics and Astrophysics, Delhi University
20. Zhang Y, Du G, Liu D, Wang X, Ma Y, Wang J, Yin J, Yang X, Hou X, Yang S (2002) J Crys Growth 243:439
21. Lu YM, Hwang WS, Liu WY, Yang JS (2001) Mater Chem Phys 72:269
22. Nakata Y, Okada T, Maeda M (2002) Appl Surf Sci 197/198:368
23. Kang DJ, Kim JS, Jeong SW, Roh Y, Jeong SH, Boo JH (2005) Thin Solid Films 475:160
24. Maissel LI, Glang R (1970) In: Handbook of thin film technology. McGraw-Hill Book Company, New York, pp 4–15
25. Kim NH, Kim HW (2004) Brit Ceram Trans 103:15
26. Ondo-ndong R, Ferblantier G, Al Kalfioui M, Boyer A, Foucaran A (2003) J Cryst Growth 255:130
27. Tarte P (1961) Spectrochim Acta 18:467
28. Kao KC, Hwang W (1981) In: Electrical transport in solids. Pergamon Press, Oxford, England, pp 150
29. Chu SY, Water W, Liaw JT (2003) J Euro Ceram Soc 23:1593
30. Mitsuyu T, Ono S, Wasa K (1980) J Appl Phys 51(5):2464
31. Subramanyam TK, Naidu BS, Uthanna S (1999) Cryst Res Technol 34:981